

Techniques and Considerations for Driving Piezoelectric Actuators at High-speed

Andrew J. Fleming

School of Electrical Engineering and Computer Science, The University of Newcastle,
Australia.

ABSTRACT

Due to their high stiffness, small dimensions and low mass, piezoelectric stack actuators are capable of developing large displacements with bandwidths of greater than 100 kHz. However, due to their large electrical capacitance, the associated driving amplifier is usually limited in bandwidth to a few kHz.

In this paper the limiting characteristics of piezoelectric drives are identified as the signal-bandwidth, output-impedance, cable inductance, and power dissipation. A new *dual-amplifier* is introduced that exhibits a bandwidth of 2 MHz with a 100 nF capacitive load. Experiments demonstrate a 20 V 300 kHz sine wave being applied to a 100 nF load with negligible phase delay and a peak-to-peak current of 3.8 A. Although the peak output voltage and current is 200 V and 1.9 A, the worst-case power dissipation is only 30 W.

1. INTRODUCTION

Piezoelectric transducers are the actuator of choice in applications requiring precision motion and force control. They are compact, light-weight, and high in stiffness. These properties permit high mechanical resonance frequencies, typically in the tens or hundreds of kilohertz.

Many applications utilize the high-speed and precision offered by piezoelectric actuators. Examples include nano-fabrication systems [1] [2], high-speed micro-mechanical systems [3], Scanning Probe Microscopes (SPMs) [4], and vibration control systems [5] [6] [7].

Both scanning probe microscopes and nano-fabrication systems use piezoelectric tube or stack based scanners for sample positioning and probe control. With increasing SPM imaging speed and nano-fabrication throughput, greater demands are placed on the bandwidth of the positioning stages [8]. These demands have necessitated the use of small, high capacitance, multi-layer actuators to achieve the required stiffness and resonance frequency [9] [10].

Unfortunately, due to the high capacitance of stacked and multi-layer actuators, in practice, system bandwidth is usually dictated by driving electronics. The first contribution of this paper is to identify the limitations of piezoelectric drive electronics. The foremost limitations established in the following section are signal bandwidth, output impedance, cable inductance and power dissipation.

To circumvent the limitations identified, a new amplifier is proposed in Section 3. The proposed *dual-amplifier* comprises a standard high-voltage amplifier and secondary low-voltage amplifier to increase performance at high frequencies. Experimental results in Section 4 demonstrate a bandwidth of 2 MHz with a 100 nF load capacitance.

2. BANDWIDTH LIMITATIONS

2.1. Passive bandwidth limitations

Two major causes of bandwidth limitation are the amplifiers output impedance and the inductance of cables and connectors. Consider the electrical circuit shown in Figure 1, where a voltage source is connected to a piezoelectric actuator. The actuator is modeled as a capacitance C_p in series with a strain dependent voltage source V_p . The resistance R_s and inductance L are the source impedance and cable inductance respectively.

E-mail: andrew.fleming@newcastle.edu.au

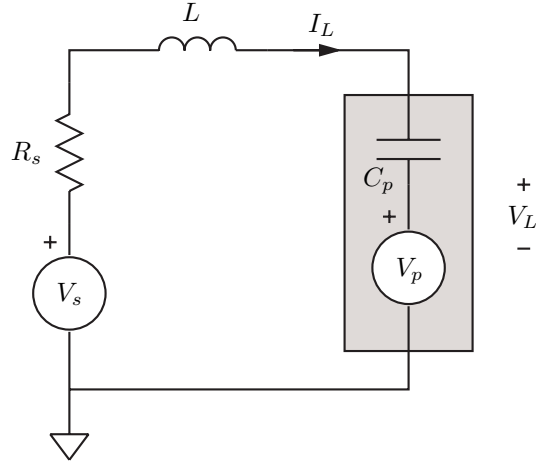


Figure 1. A voltage source V_s driving a piezoelectric load. The actuator is modeled by a capacitance C_p and strain dependent voltage source V_p . The resistance R_s and inductance L are the output impedance and cable inductance respectively.

(a) Bandwidth due to R_s				(b) Resonance frequency due to L			
	C_p				C_p		
R_s	100 nF	1 uF	10uF	L	100 nF	1 uF	10uF
1 Ω	1.6 MHz	160 kHz	16 kHz	25 nH	3.2 MHz	1 MHz	320 kHz
10 Ω	160 kHz	16 kHz	1.6 kHz	250 nH	1 MHz	320 kHz	100 kHz
100 Ω	16 kHz	1.6 kHz	160 Hz	2500 nH	320 kHz	100 kHz	32 kHz

Table 1. Bandwidth limitation imposed by source impedance (a) and cable inductance (b)

The cable inductance per meter L_m can be calculated from the characteristic impedance Z_0 and capacitance per meter C_m using the equation [11]:

$$L_m = Z_0^2 C_m. \quad (1)$$

The inductance of standard RG-58 coaxial cable is 250 nH/m, this is lower than typical speaker cable which has an inductance of around 600 nH/m. Both are commonly used as interconnects between amplifiers and actuators.

The amplifier source impedance refers to the high frequency output impedance of the amplifier. In commercially available amplifiers, R_s is typically between 10 and 100 ohms. When considering the effects of both output impedance and cable inductance, the transfer function from source voltage V_s to load voltage V_L is:

$$\frac{V_L(s)}{V_s(s)} = \frac{\frac{1}{LC_p}}{s^2 + \frac{R_s}{L}s + \frac{1}{LC_p}}. \quad (2)$$

This is a unity-gain second-order resonant low-pass filter with resonance frequency f_r and damping ratio ξ defined by:

$$f_r = \frac{1}{2\pi\sqrt{LC_p}}, \quad \xi = \frac{R_s\sqrt{LC_p}}{2L}. \quad (3)$$

If inductance is neglected, the first-order cut-off frequency resulting from the source resistance is

$$f_c = \frac{1}{2\pi R_s C_p}. \quad (4)$$

In Table 1 the first-order cut-off frequency and resonance frequency is tabulated for a range of typical values for R_s , C_p and L . Clearly, the output impedance is of primary concern. This is because the bandwidth imposed

f	C_p		
	100 nF	1 uF	10uF
30 Hz	0.19 mA	1.9 mA	19 mA
3 kHz	19 mA	190 mA	1.9 A
300 kHz	1.9 A	19 A	190 A

Table 2. Minimum current requirements for a 10 V sinusoid

by source impedance is inversely proportional to both resistance and capacitance. Reductions in both of these parameters can achieve significant bandwidth improvements. Alternatively, the resonance frequency is inversely proportional to both \sqrt{L} and $\sqrt{C_p}$, so a four fold reduction in L or C_p is required to double the bandwidth.

Although it is difficult to achieve improvements in resonance frequency, all effort should be expended in doing so, as a lightly damped resonance in the transfer function is highly undesirable. In addition to oscillation induced by wide band input signals, the gain peaking and phase lag can severely limit the performance of feedback control systems in which the amplifier and actuator are enclosed.

2.2. Amplifier bandwidth

The most obvious bandwidth limitation is the small-signal bandwidth of the amplifier. In commercial devices, this can range from 10 kHz to 100 kHz. Unfortunately, these figures are load dependent. The highly capacitive impedance and resonant nature of piezoelectric loads introduces phase-lag into the feedback path. This reduces bandwidth, decreases phase-margin and can lead to instability. For standard voltage-feedback amplifiers with dominant pole compensation, a rough rule of thumb is that closed-loop bandwidth cannot exceed one tenth the cut-off frequency of the pole formed by the amplifiers output impedance R_s and load capacitance C_p . Typical frequencies for this pole are shown in Table 1 (a). Thus, with standard voltage-feedback amplifiers, the dominant limitation is the output pole. To improve performance, this pole will either have to be increased in frequency, or removed from the closed-loop transfer function of the amplifier, or both.

Further bandwidth restrictions are imposed by the maximum slew rate of the amplifier. This is the maximum rate at which the output voltage can change and is usually expressed in Volts per microsecond $V/\mu s$. For sinusoidal signals, the amplifiers slew rate must exceed

$$SR_{\sin} = V_{p-p}\pi f, \quad (5)$$

where V_{p-p} is the peak-to-peak voltage and f is the frequency. Triangular signals, used in scanning systems require a lesser slew rate of

$$SR_{\text{tri}} = V_{p-p}2f. \quad (6)$$

If a 300 kHz sine-wave is to be reproduced with an amplitude of 10 V, the required slew rate is 20 $V/\mu s$. This value is proportional to both frequency and amplitude. Although slew rate limitations can be critical when considering resistive or inductive loads; when dealing with capacitive loads, the current-limit is usually exceeded well before the slew rate limit. This is discussed in the following section.

2.3. Current and power limitations

Neglecting the piezoelectric strain voltage, i.e. when driving the actuator off-resonance, the current delivered to a piezoelectric actuator is approximately

$$I_L(s) = V_L(s)C_p s, \quad (7)$$

or in the time domain

$$I_L(t) = C_p \frac{d V_L(t)}{dt}. \quad (8)$$

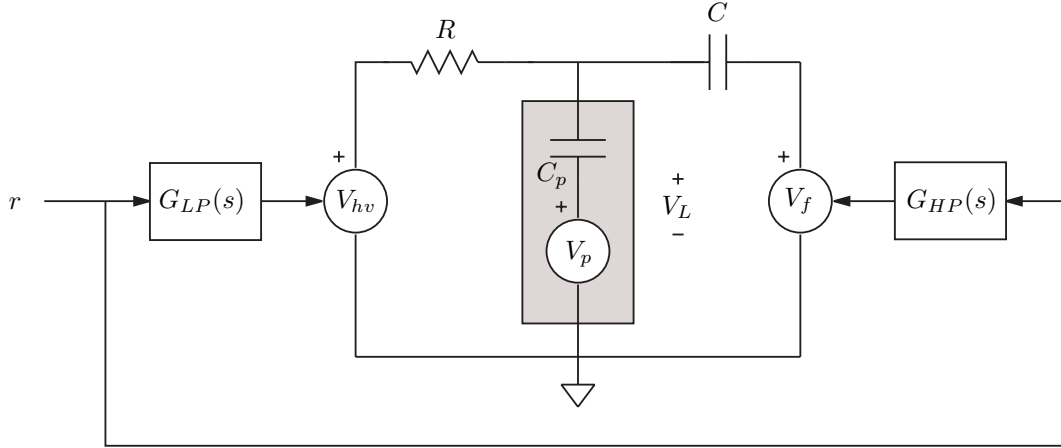


Figure 2. Schematic diagram of a high-speed dual-amplifier. The reference input r is applied simultaneously to a slow high-voltage amplifier V_{hv} , and a fast low-voltage amplifier V_f . The two amplifiers are coupled to the load through the resistance R and capacitance C .

For sinusoidal signals, the maximum positive and negative current is equal to

$$I_L^{\max} = V_{p-p}\pi f C_p. \quad (9)$$

For triangular signals, the maximum current is

$$I_L^{\max} = V_{p-p}2f C_p. \quad (10)$$

Examples of current requirements for different load capacitances and frequencies are shown in Table 2.

When selecting the required current-limit of an amplifier, the key parameter is the maximum allowable power dissipation. The power dissipation in the output stage of a linear amplifier is equal to the product of current through, and voltage across the power transistors. That is, the power dissipation P_d is

$$P_d = I_L(V_{rail} - V_L), \quad (11)$$

where V_{rail} the is the internal power supply voltage.

In an amplifier designed to tolerate output short circuits, i.e. $V_L = 0$, the maximum power dissipation typically sets the limit on maximum allowable output current. Fold-back current limiting can increase maximum output current but is not suitable for capacitive loads where maximum current can be required with low or no output voltage.

3. DUAL AMPLIFIER

3.1. Circuit operation

High voltage amplifiers cannot achieve bandwidths over 100 kHz with large capacitive loads for two main reasons. First, the output impedance of high-voltage output stages is typically around $10 \Omega^*$, this limits the small signal bandwidth to the values shown in Table 1 (a) with $R_s = 10 \Omega$. Second, the power dissipation, even for output voltages as low as 10V, is in the hundreds of Watts at frequencies above 100 kHz. For these reasons, high-voltage amplifiers driving capacitive loads of 100 nF or greater are usually restricted in bandwidth to around 10 kHz.

*Due to second-breakdown in bipolar transistors [11], MOSFET transistors are the only option in high-voltage circuits where power dissipation of greater than a few Watts is required. The best output impedance at high-frequencies is obtained by a complementary class AB MOSFET push-pull stage. Although Class A stages achieve the lowest output impedance, they are impractical due to their low efficiency and high quiescent dissipation [11].

In this work, a new amplifier is presented that alleviates the problems of high-voltage amplifiers by adding an auxiliary low-voltage stage to improve output impedance and drop power dissipation at high frequencies. A schematic diagram of the *dual-amplifier* is shown in Figure 2. Essentially the dual-amplifier comprises two amplifiers, a standard high-voltage amplifier V_{hv} and a fast low-voltage amplifier V_f . The low-voltage stage drives the actuator at high-frequencies but with reduced range. Due the lower supply voltage (say ± 15 V) the low-voltage stage dissipates less power and can use bipolar transistors under heavy forward bias to provide an output impedance in the milliOhm range.

The two amplifier are coupled to the load through the resistor R and capacitor C . This network ensures that the load voltage V_L receives low-frequency power from V_{hv} and high-frequency power from V_f . As a function of V_{hv} and V_f , the load voltage is equal to

$$V_L(s) = \frac{\alpha}{s + \alpha} V_{hv}(s) + \frac{C}{C + C_p} \frac{s}{s + \alpha} V_f(s) \quad \text{where, } \alpha = \frac{1}{R(C + C_p)}. \quad (12)$$

That is, the response from the high-voltage side is a low-pass filter, while the response from the low-voltage side is a high-pass filter with attenuation. A key observation is that the filters $\frac{\alpha}{s + \alpha}$ and $\frac{s}{s + \alpha}$ are complementary, i.e. if the attenuation due to C and C_p is accounted for, a signal applied to both amplifiers will be perfectly reproduced across the load. Low frequency power is supplied by V_{hv} while high frequency power is supplied by V_f , which is exactly the situation desired.

A design issue for the circuit shown in Figure 2 is the choice of R and C . Choosing C is straight forward. C should be chosen so that the ratio $\frac{C}{C + C_p}$ is close to unity and that the combination of C and C_p does not unnecessarily load the high-voltage stage. A reasonable compromise is $C = 10C_p$. With C fixed, the selection of R controls the low and high-pass cutoff frequencies. A good choice is to design the cut-off frequency and R so that the high-voltage amplifier can be fully utilized, that is, so that at the cut-off frequency, the high-voltage amplifier is about to reach current-limit. If the peak-to-peak voltage and current from the high-voltage stage is V_{pp} and I_{pp} , the corresponding impedance Z is

$$\frac{V_{pp}}{I_{pp}} = Z = \left| R + \frac{-j}{2\pi f(C + C_p)} \right| \quad (13)$$

$$\frac{V_{pp}}{I_{pp}} = \sqrt{R^2 + \frac{1}{4\pi^2 f^2 (C + C_p)^2}} \quad (14)$$

The frequency where this occurs can be set to the filter cutoff frequency by substituting $f = \frac{\alpha}{2\pi}$. Simplification yields

$$\frac{V_{pp}}{I_{pp}} = \sqrt{2R^2}. \quad (15)$$

Hence, R and the cutoff frequency in Hertz F_c are

$$R = \sqrt{\frac{1}{2} \left(\frac{V_{pp}}{I_{pp}} \right)^2} \quad F_c = \frac{1}{2\pi R(C + C_p)}. \quad (16)$$

3.2. Range considerations

Although the low-voltage stage significantly improves high-frequency performance, it is important to note that the penalty is reduced range at high-frequencies. However, in many applications this does not present a significant drawback as there is no requirement to drive the actuator at full range above 100 kHz. Indeed, the majority of piezoelectric stack actuators would be destroyed by inertial forces and dielectric heating.

The full voltage range of the amplifier can only be realized within the bandwidth of the high-voltage stage, i.e. from DC to $\frac{\alpha}{2\pi}$ Hz. More precisely, the full voltage range is reduced by $\frac{1}{\sqrt{2}}$ at $\frac{\alpha}{2\pi}$ Hz.

To avoid saturation of the low-voltage stage in the frequency band where full range is available, the additional first-order complementary filters $G_{HP}(s)$ and $G_{LP}(s)$ shown in Figure 2 are required. While $G_{HP}(s)$ removes



Figure 3. Amplifier enclosure with connected cable and 100 nF capacitive load

low frequency signal content to avoid saturation of the low voltage stage, $G_{LP}(s)$ ensures that both stages remain complementary.

The cut-off frequency is determined by the difference in range between the high- and low-voltage stages. $G_{HP}(s)$ should be high enough in frequency to ensure that the range of the low-voltage stage is not exceeded at $\frac{\alpha}{2\pi}$ Hz. For example, if the low-voltage stage has one-tenth the range of the high-voltage stage, the cut-off frequency should be ten times greater than the RC cutoff in (12), i.e.

$$G_{HP}(s) = \frac{s}{s + \beta} \quad \text{where } \beta = 10\alpha. \quad (17)$$

Once $G_{HP}(s)$ is decided, the filter $G_{LP}(s)$ is calculated to maintain complimentary signal paths through the low- and high-voltage stages. It is easily verified that this condition is satisfied when

$$G_{LP}(s) = \frac{s + \alpha}{a} \left(1 - \frac{s}{s + \beta} \frac{s}{s + \alpha} \right) = \frac{(\beta + \alpha)}{\alpha} \frac{s + \frac{\beta\alpha}{\beta + \alpha}}{s + \beta} \quad (18)$$

The output range versus frequency of the dual-amplifier can be estimated from the dominant poles in the system and the range of the low- and high-voltage stages. That is,

$$\text{Range}(\omega) = \left| \frac{\alpha}{s + \alpha} R_{HV} + \frac{s}{s + \beta} R_{LV} \right|_{s=j\omega} \quad (19)$$

where R_{HV} and R_{LV} are the full output voltage ranges of the high- and low-voltage stages.

4. ELECTRICAL DESIGN

In this section the implementation of a dual-amplifier is described. The goal is to drive a 100 nF load with a full voltage range of 0-200 V, and a high-frequency range of 20 V peak-to-peak. The completed device is pictured in Figure 3.

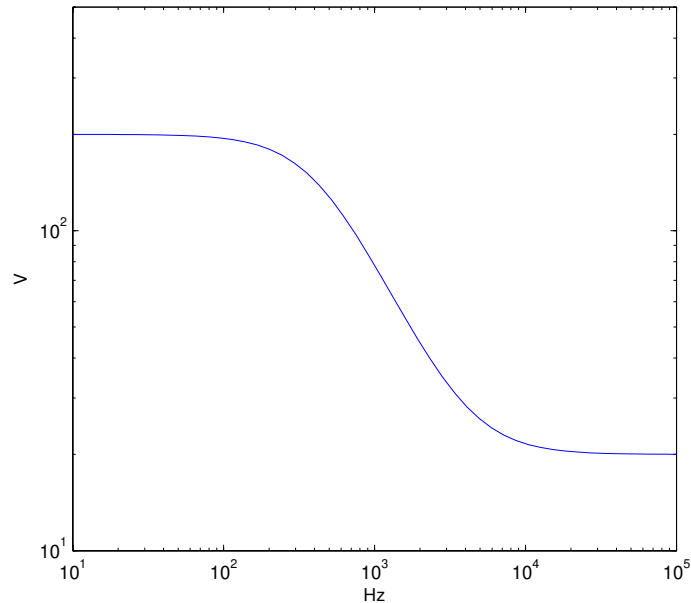


Figure 4. The peak-to-peak output voltage range of the dual-amplifier.

4.1. High-voltage stage

The high-voltage stage is a basic voltage-feedback amplifier constructed from an Apex Microtechnology PA98 450 V op amp. This is supplied by an International Power IHB200-0.12 215 V power supply with a current rating of 120 mA. With sufficient storage capacitance, the 120mA output current is sufficient to supply the PA98 with its required 20 mA quiescent current and allow for an amplifier current-limit of ± 200 mA so long as the load is capacitive. The worst case power dissipation into a capacitive load is 20 W, safely within the rated limit of 30 W.

As discussed in Section 3.1, a load capacitance of 100 nF requires a filter capacitance C of approximately $1 \mu\text{F}$. R can be calculated from equation 16 as 353Ω . The resulting filter cutoff frequency is 409 Hz.

To avoid saturation of the low-voltage stage, which has only one-tenth the high-voltage range, the filter cutoff frequency of $G_{HP}(s)$ should be approximately 5 kHz, i.e. $\beta = 2\pi 5000$. As discussed in Section 3.2, the resulting range versus frequency is plotted in Figure 4.

4.2. Low-voltage stage

The necessary amplifier performance requirements for achieving high bandwidth with capacitive loads were identified in Sections 2.1 and 2.2. With a 100 nF load, a 1 MHz bandwidth requires an output impedance of less than 1Ω and a small-signal bandwidth well in excess of 1 MHz.

With high-voltage supplies and MOSFET output transistors, low output impedance is extremely difficult to achieve. However, due to the reduced supply voltage, high-performance bipolar transistors can be utilized. These transistors can be operated under heavy forward bias to drop the output impedance to well below 1Ω .

The schematic of a wide-bandwidth low-voltage amplifier is shown in Figure 5. This circuit utilizes a high-speed op amp to achieve the gain of 21 and bandwidth in excess of 10 MHz. The following biasing stage provides drive for the output transistors and protects the op amp from excessive current load. The output transistors are high-performance audio types and provide excellent linearity in open-loop. With sufficient bias, the output stage is sufficiently linear to negate the need for output voltage feedback. This is a major advantage as the gain stage is not limited in bandwidth by the pole formed by the output impedance and load capacitance.

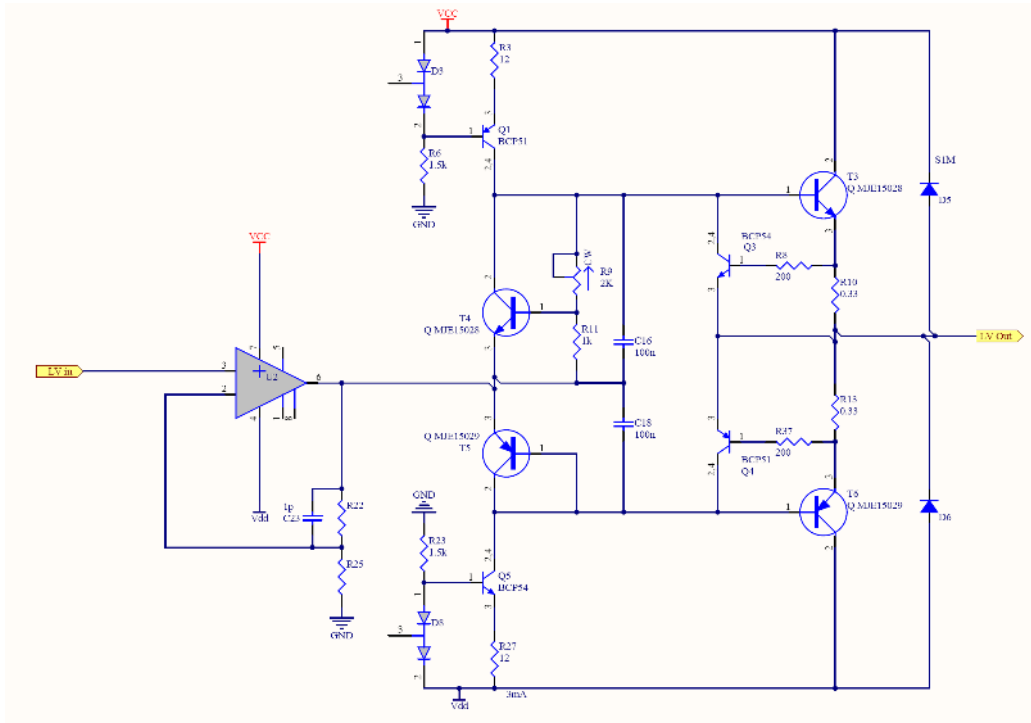


Figure 5. Schematic of the low-voltage amplifier stage. This stage comprises an op amp amplifier to achieve the correct signal gain followed by a bipolar class AB output.

A further advantage of the low-voltage stage is that it can provide large output currents at high frequency without major power dissipation. For example, a 300 kHz 20 V peak-to-peak sine with 100 nF load requires 1.9 A peak current. With a 2 A current limit, the worst-case power dissipation is around 30 W. In comparison, a 200 V amplifier would dissipate 400 W in the same scenario, which is highly impractical.

With the high- and low-voltage stages complete, the assembled dual-amplifier was tested for frequency response and drive capability with a 100 nF load. In Figure 6, the amplifier’s response to a 300 kHz 20 V peak-to-peak sine wave is plotted. The phase-lag between input and output is extremely low. The frequency response is plotted in the next section after a discussion of cable and interconnect inductance.

4.3. Cabling and interconnects

In Section 2.1 the cable inductance was identified as a major limitation of amplifier bandwidth when driving highly capacitive loads. As cable inductance is proportional to the area enclosed in the loop between the two conductors, it is desirable to position the conductors as closely together as possible. Simply using twisted small diameter wire is not sufficient as the resistance of the conductors is also of importance. A better solution is to use copper foil for each conductor separated by a thin insulating layer, this configuration yields minimal loop area, low resistance and low characteristic impedance (1).

Cables with the geometry discussed above have been developed for audio applications, one manufacturer is Alphacore. The MI-2 cable pictured in Figures 3 and 7 contains two copper foil conductors, a Polyester dielectric and a Polycarbonate outer layer. The width and thickness is 9.5×0.254 mm which provides a satisfactory resistance of 14 mΩ per meter. Thanks to the high dielectric strength of the insulator, the conductors are separated by only 76 μm which results in a cable inductance of only 33 nH per meter, approximately an order of magnitude less than RG-58 coaxial cable (which is 250 nH/m).

The inductance of connectors between the cable and amplifier is also of importance. In this work, to minimize loop area, the cable is connected directly to the amplifier circuit board by bolting or soldering it to the exposed

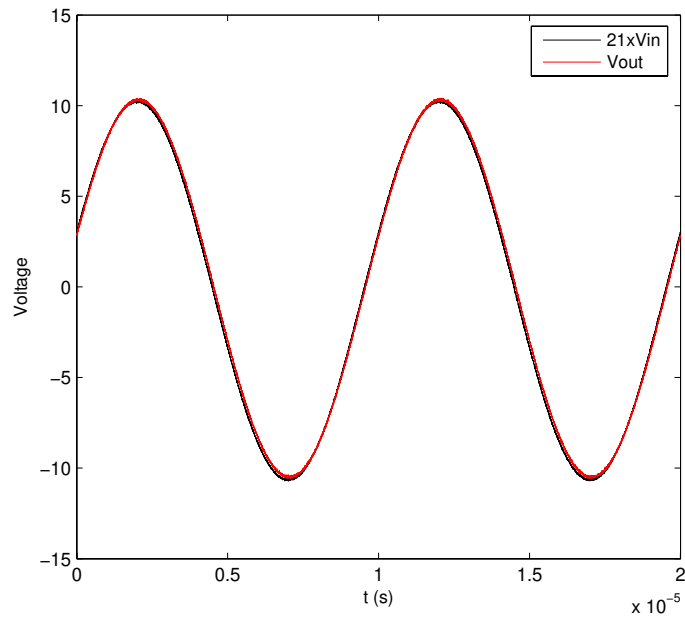


Figure 6. Measured amplifier input and output with a 300 kHz sine wave reference and 100 nF load. The peak-to-peak current is 3.8A.



Figure 7. Close-up of low-inductance connection between amplifier circuit board and cable

traces on the top and bottom surfaces. This configuration is pictured in Figure 7 where a nylon bolt is used to fix the cable onto the PCB.

The frequency response from amplifier input to load voltage is plotted in Figure 8. With no load, the amplifier bandwidth is exceptional at around 8 MHz. With a 100 nF load and a standard 50 Ω coaxial cable, a cable resonance appears at 350 kHz. In contrast, the resonance frequency with MI-2 cable is 1.5 MHz.

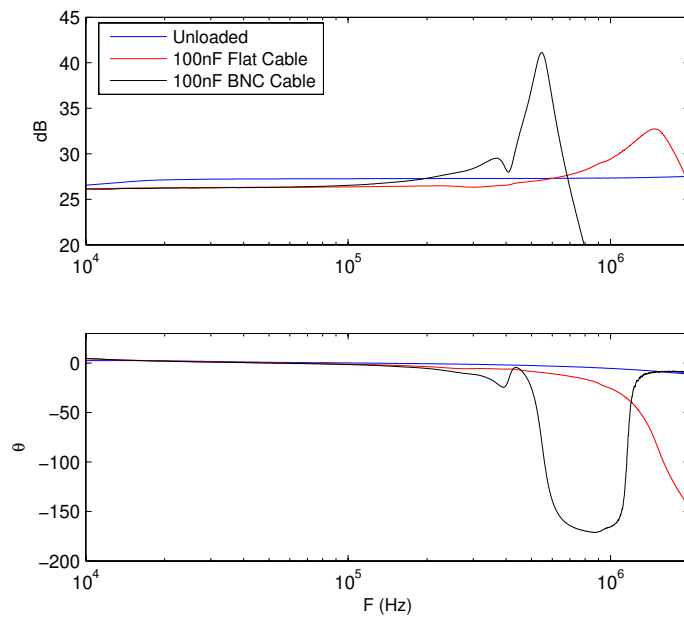


Figure 8. Amplifier frequency response with open-circuit and capacitive loads

5. CONCLUSIONS

In this work the bandwidth limitations of standard piezoelectric drives were identified as:

- High output impedance
- The presence of a pole in the voltage-feedback loop due to output impedance and load capacitance
- Insufficient current capacity due to power dissipation
- High cable and connector inductance

These limitations were overcome by combining a standard high-voltage amplifier with a fast low-voltage stage. Due to the lesser supply voltage of the low-voltage amplifier, it was possible to utilize a heavily biased bipolar output stage to provide low output impedance. The low supply voltage also allows an order of magnitude increase in output current with no significant increase in power or dissipation requirements.

Cable and interconnect inductance proved to be the greatest limitation to bandwidth. A flat foil cable with ultra-low inductance was proposed for maximum bandwidth.

The completed amplifier's bandwidth, with 100 nF load was measured at 2 MHz. The main limitation was a cable resonance at 1.5 MHz. The device was demonstrated to drive a 100 nF load with a 300 kHz 20 V peak-to-peak sine wave with negligible phase-lag. Although peak-to-peak current was 3.8 A, the worst case power dissipation is only 30 Watts.

REFERENCES

1. A. A. Tsenga, A. Notargiacomob, and T. P. Chen, "Nanofabrication by scanning probe microscope lithography: A review," *Journal of Vacuum Science and Technology* **23**, pp. 877–894, May/June 2005.
2. F. J. Rubio-Sierra, W. M. Heckle, and R. W. Stark, "Nanomanipulation by atomic force microscopy," *Advanced Engineering Materials* **7**(4), pp. 193–196, 2005.
3. K. Uchino and J. R. Giniewica, *Micromechatronics*, Marcel Dekker Inc., New York, 2003.
4. D. Bonnell, ed., *Scanning probe microscopy and spectroscopy. Theory, Techniques, and Applications. Second Edition.*, Wiley-VCH, Hoboken, NJ, 2001.
5. D. J. Inman, *Vibration with control*, John Wiley and Sons Ltd., Chichester, England, 2006.
6. A. Preumont, *Mechatronics, Dynamics of electromechanical and piezoelectric systems*, Springer, 2006.
7. S. O. R. Moheimani and A. J. Fleming, *Piezoelectric Transducers for Vibration Control and Damping*, Springer-Verlag, 2006.
8. Q. Zou, K. K. Leang, E. Sadoun, M. J. Reed, and S. Devasia, "Control issues in high-speed AFM for biological applications: collagen imaging example," *Asian Journal of Control* **6**, pp. 164–176, June 2004.
9. G. Schitter, K. J. strm, B. E. DeMartini, P. J. Thurner, K. L. Turner, and P. K. Hansma, "Design and modeling of a high-speed AFM-scanner," *IEEE Transactions on Control Systems Technology* **15**, pp. 906–915, September 2007.
10. M. J. Rost, L. Crama, P. Schakel, E. van Tol, G. B. E. M. van Velzen-Williams, C. F. Overgaw, H. ter Horst, H. Dekker, B. Okhuijsen, M. Seynen, A. Vijftigschild, P. Han, A. J. Katan, K. Schoots, R. Schumm, W. van Loo, T. H. Oosterkamp, and J. W. M. Frenken, "Scanning probe microscopes go video rate and beyond," *Review of Scientific Instruments* **76**, pp. 053710–1–053710–9, April 2005.
11. P. Horowitz and W. Hill, *The art of electronics*, Cambridge University Press, Cambridge, UK, 1989.